

Ni–Zn ferrite films with high resonance frequency in the gigahertz range deposited by magnetron sputtering at room temperature

This article has been downloaded from IOPscience. Please scroll down to see the full text article.

2009 J. Phys. D: Appl. Phys. 42 125006

(<http://iopscience.iop.org/0022-3727/42/12/125006>)

View [the table of contents for this issue](#), or go to the [journal homepage](#) for more

Download details:

IP Address: 210.26.48.58

The article was downloaded on 07/06/2010 at 03:38

Please note that [terms and conditions apply](#).

Ni–Zn ferrite films with high resonance frequency in the gigahertz range deposited by magnetron sputtering at room temperature

Dangwei Guo, Zhengmei Zhang, Min Lin, Xiaolong Fan, Guozhi Chai, Yan Xu and Desheng Xue¹

Key Laboratory for Magnetism and Magnetic Materials of the Ministry of Education, Lanzhou University, Lanzhou 730000, People's Republic of China

E-mail: xueds@lzu.edu.cn

Received 10 January 2009, in final form 21 April 2009

Published 5 June 2009

Online at stacks.iop.org/JPhysD/42/125006

Abstract

$\text{Ni}_x\text{Zn}_{1-x}\text{Fe}_2\text{O}_4$ ($0.28 \leq x \leq 0.70$) thin films with well-crystallized spinel structure and thickness $\sim 1.5 \mu\text{m}$ were prepared by radio frequency magnetron sputtering at room temperature on Si(1 1 1) substrates. The complex permeability $\mu = \mu' - i\mu''$ values of as-deposited films were measured at frequencies up to 5.5 GHz. With increasing Ni content x the real part of the permeability μ' decreased from 20.5 to 7, while the resonance frequency f_r increased from 1.85 up to 4.3 GHz. Film with optimized $x = 0.45$ exhibited a large μ' of 15 and μ'' of 21 at an f_r of 2.8 GHz. It was noted that all the films exhibited very high f_r exceeding Snoek's limit value of the ferrite bulk specimen, and the reason was investigated preliminarily.

(Some figures in this article are in colour only in the electronic version)

1. Introduction

Recently, due to the ongoing trend for miniaturization and steadily increasing operating frequencies into the gigahertz range of electronic devices, soft magnetic ferrite films with high resistivity and resonance frequency have been in critical demand for high frequency applications such as planar inductors, micro-transformers and electromagnetic interference (EMI) suppressors [1–5]. For these kinds of applications a lower temperature deposition process is highly advantageous, because the soft ferrite films must be deposited on such substrates as circuit boards, metal wires/films and semiconductor apparatus [6–8]. To our knowledge, soft ferrite films deposited by pulsed laser deposition (PLD) [9, 10], sputtering [11–13], sol–gel [14], etc require high temperature post-heating treatments or substrate heating at least of 600 °C to obtain a better spinel structure and soft magnetic properties, which is incapable for electronic circuit integrations.

It is noted that the research groups of Abe and Matsushita have prepared Ni–Zn(–Co) ferrite films with well-crystallized spinel structure and high resistivity by spin-spray ferrite plating at $T = 90^\circ\text{C}$, and they exhibited a large permeability μ' of 30–50 and high resonance frequency f_r in the gigahertz range [6, 8]. It is well known that magnetron sputtering as a versatile physical technique of depositing films has a major advantage compared with the chemical methods. The preparation condition and the chemical composition of the films could be better controlled, and the films deposited have fine compactness and little defect. Therefore, it is desirable that soft ferrite films with well-defined spinel structure and excellent high frequency magnetic properties are deposited by magnetron sputtering at lower temperature.

In this work, $\text{Ni}_x\text{Zn}_{1-x}\text{Fe}_2\text{O}_4$ ($0.28 \leq x \leq 0.70$) ferrite films with spinel crystal structure were successfully fabricated without any heating treatments by magnetron sputtering, and their structural and magnetic characteristics as well as the complex permeability $\mu = \mu' - i\mu''$ were investigated. Films

¹ Author to whom any correspondence should be addressed.

with a large saturation magnetization of $365.1 \text{ emu cm}^{-3}$, a high frequency property of $\mu' = 15$ and an $f_r = 2.8 \text{ GHz}$ can be obtained at the composition of $\text{Ni}_{0.45}\text{Zn}_{0.55}\text{Fe}_2\text{O}_4$.

2. Experimental procedure

$\text{Ni}_x\text{Zn}_{1-x}\text{Fe}_2\text{O}_4$ ($0.28 \leq x \leq 0.70$) ferrite films with thickness $\sim 1.5 \mu\text{m}$ were deposited onto $10 \times 10 \text{ mm}^2$ Si(1 1 1) substrates attached to a water-cooling system by radio frequency (RF) magnetron sputtering at room temperature with a base pressure lower than $2 \times 10^{-5} \text{ Pa}$. A $\text{Ni}_{0.5}\text{Zn}_{0.5}\text{Fe}_2\text{O}_4$ ferrite target, 76 mm in diameter and 3 mm in thickness, on which NiFe_2O_4 and ZnFe_2O_4 ferrite chips were placed in a regular manner, was used. We have prepared Ni–Zn ferrite films with different compositions by varying the numbers of NiFe_2O_4 and ZnFe_2O_4 chips. The RF power density was 4.4 W cm^{-2} and a mixed gas of argon (Ar) and oxygen (O_2) was used during sputtering. The sputtering pressure was kept at 2.0 Pa, while the proportion of O_2 pressure to the total pressure was 20%.

The compositions of the ferrite films were measured by energy dispersive x-ray spectroscopy (EDS). The crystallographic and microstructure properties of the ferrite films were characterized by x-ray diffraction (XRD, Philips X'Pert PRO with $\text{Cu K}\alpha$ radiation) and a field emission scanning electron microscope (SEM, Hitachi S-4800), respectively. The static magnetic measurements of the films were performed by using a vibrating sample magnetometer (VSM, Lakeshore 7304 model). The saturation magnetization (M_s) and coercivity (H_c) were evaluated from the loops of which the applied field H is parallel to the film plane. The complex permeability $\mu = \mu' - i\mu''$ of the ferrite films were measured by a PNA E8363B vector network analyzer using the shorted microstrip transmission-line perturbation method from 170 MHz to 5.5 GHz [15]. All the above observations and measurements were performed on as-deposited samples at room temperature.

3. Results and discussion

EDS analysis of the films quantifies the relative ferrite composition. The results are found to be close to the expected chemical formula $\text{Ni}_x\text{Zn}_{1-x}\text{Fe}_2\text{O}_4$ with $x = 0.28, 0.38, 0.45, 0.60$ and 0.70 . Figure 1 shows the XRD patterns of the as-deposited $\text{Ni}_x\text{Zn}_{1-x}\text{Fe}_2\text{O}_4$ ($0.28 \leq x \leq 0.70$) thin films at room temperature. It shows that all the samples are well crystallized and are in single phase with a spinel crystal structure. The main peak is the (3 1 1) peak and no preferential orientation appears in all the films, which is in agreement with other reports [2, 6, 12, 13]. It can be seen that with increasing Ni concentration x the (3 1 1) peaks shift to large diffraction angles, which reveals that for the thin films with more Ni content the lattice parameters are less. The lattice parameters a (Å) of the ferrite films obtained from the XRD patterns are also shown in figure 1. We attribute this to the different radius of Ni (0.78 \AA) and Zn (0.82 \AA), which means that the more the Ni ions the less the lattice parameters.

The surface and cross-sectional SEM images of the as-deposited ferrite film, with $x = 0.45$ as a typical case,

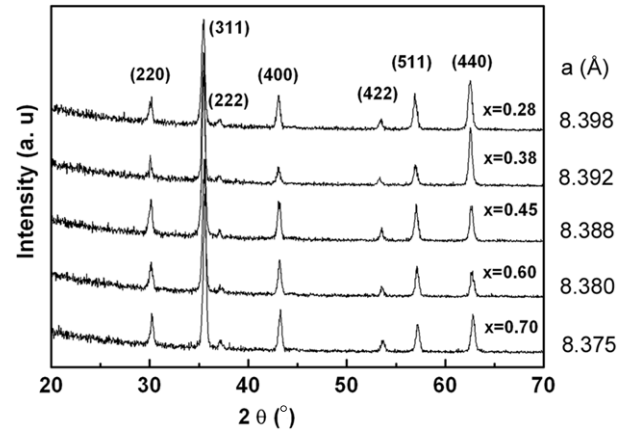


Figure 1. XRD patterns of the $\text{Ni}_x\text{Zn}_{1-x}\text{Fe}_2\text{O}_4$ thin films with different Ni content x . Indices show those for the spinel structure.

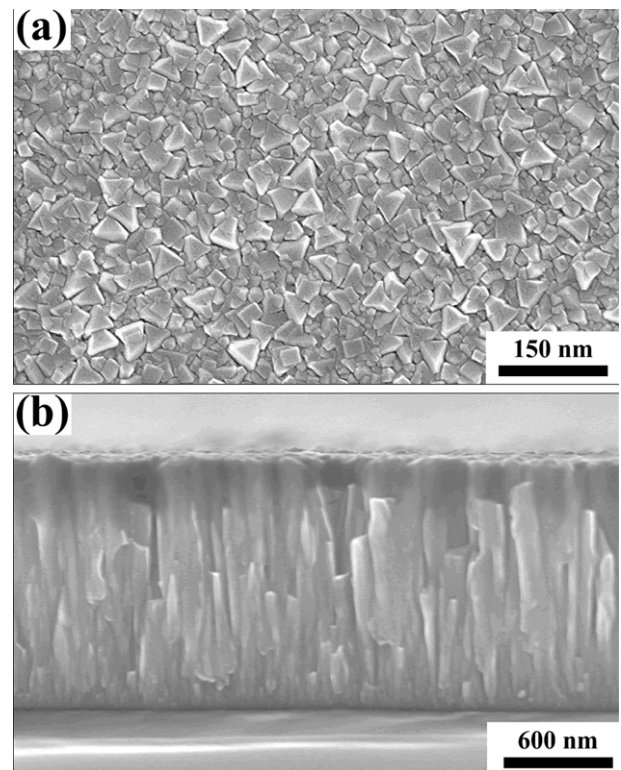


Figure 2. SEM images for the $\text{Ni}_x\text{Zn}_{1-x}\text{Fe}_2\text{O}_4$ ($x = 0.45$) thin films (a) surface topography and (b) cross-section diagram.

are shown in figures 2(a) and (b). As seen from figure 2(a), the film is composed of nanocrystalline particles which are in the range of 10–30 nm. The film has a smooth surface, a relatively good packing density and a definite columnar structure perpendicular to the film plane. The morphological characteristics of other films are almost the same as this, and all the films have nearly the same thickness of $\sim 1.5 \mu\text{m}$ which is estimated from the cross-sectional views.

Figure 3 shows the Ni content x dependence of saturation magnetization M_s and coercivity H_c of the Ni–Zn ferrite films. The dependence of the magnetic properties of the ferrite films on composition is analogous to that of bulks. As seen from figure 3, with an increase in the Ni content x , M_s of the ferrite

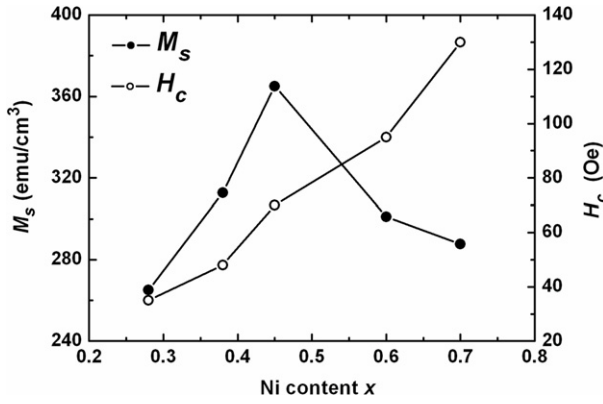


Figure 3. Dependences of M_s and H_c of the $\text{Ni}_x\text{Zn}_{1-x}\text{Fe}_2\text{O}_4$ thin films on Ni content x .

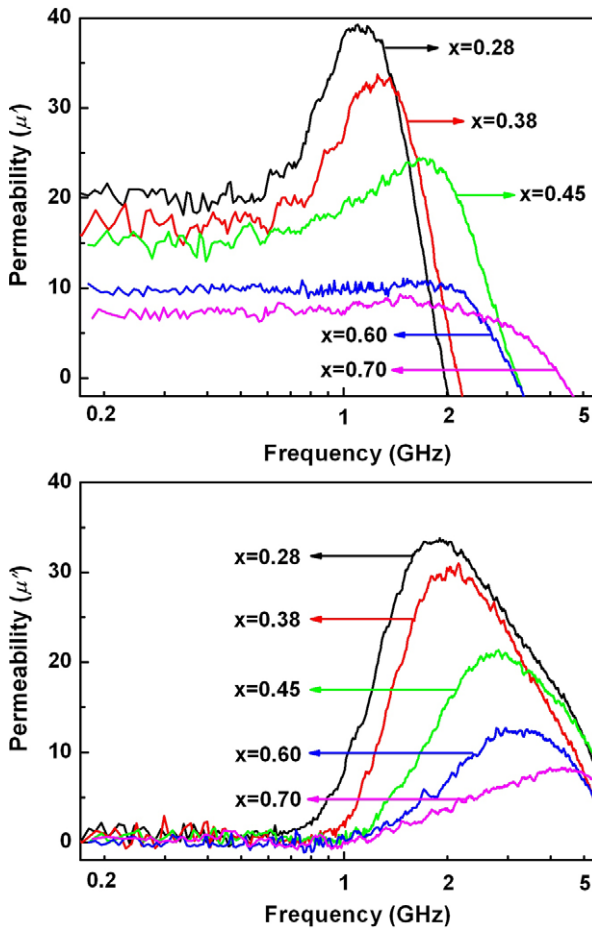


Figure 4. Complex permeability spectra for the $\text{Ni}_x\text{Zn}_{1-x}\text{Fe}_2\text{O}_4$ thin films with different Ni content x . (Colour online.)

films first increases and then decreases, while H_c increases monotonically. The variational tendency is in agreement with other reports [16]. With $x = 0.45$ M_s shows a maximum value of $365.1 \text{ emu cm}^{-3}$, which is close to that of ferrite bulks. Additionally, the increasing of H_c could be due to the increasing of the magnetocrystalline anisotropy with the increase in the Ni content x .

Figure 4 shows the frequency dependence of the complex permeability spectra for the $\text{Ni}_x\text{Zn}_{1-x}\text{Fe}_2\text{O}_4$ ($0.28 \leq x \leq 0.70$)

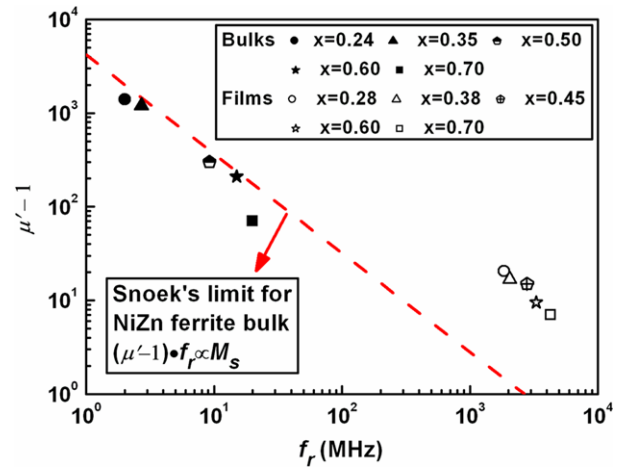


Figure 5. $\mu' - 1$ (at 170 MHz) as a function of f_r for the $\text{Ni}_x\text{Zn}_{1-x}\text{Fe}_2\text{O}_4$ thin films with different Ni content x , compared with the ferrite bulk [18, 19]. The dashed line represents Snoek's limit for the Ni–Zn ferrite bulk [6, 20].

thin films in the range of 170 MHz–5.5 GHz. The real part of the permeability μ' decreases from 20.5 to 7 with the increase in the Ni content x , while the resonance frequency f_r around which the imaginary part of the permeability μ'' reaches a maximum increases from 1.85 up to 4.3 GHz. The film with optimized $x = 0.45$ has a high μ' of 15 and f_r of 2.8 GHz because of its having a large M_s of $365.1 \text{ emu cm}^{-3}$. Especially, the film with $x = 0.70$ achieved a f_r up to 4.3 GHz, which is much higher than that in the reports about soft ferrite films [2, 4, 8, 17]. The downshift in the μ' with the increase in the Ni content x could be attributed to the increasing of Ni, which increases the effective magnetic anisotropy of the ferrite films. μ'' of all the films have large values in the gigahertz range; especially the ferrite film with $x = 0.28$ has a value of above 20 in a wide frequency range between 1.25 and 3.65 GHz and the maximum value of 33.5 at $f_r = 1.85 \text{ GHz}$.

Figure 5 shows the previously published data for the high frequency $\text{Ni}_x\text{Zn}_{1-x}\text{Fe}_2\text{O}_4$ soft ferrite bulks [18, 19] and the ferrite films in this work with different Ni content x . It is seen that the resonance frequency f_r of all the films are much higher than the ferrite bulks and exceeding Snoek's limit for the Ni–Zn ferrite bulk [6, 20]. Figure 6 shows the magnetic hysteresis loop of the as-deposited ferrite film with $x = 0.45$ as a typical case, where $H_{\text{in-plane}}$ and $H_{\text{out-of-plane}}$ denote that the applied field H is parallel and perpendicular to the film plane, respectively. The inset is the minor loop of the film with a smaller field of 60 Oe. The different shapes of the hysteresis loops in the parallel and the perpendicular directions indicate that the ferrite film exhibits obvious anisotropy and the film plane is the easy magnetizing plane.

According to the bianisotropy model presented by Xue *et al* [21] for the magnetic materials there are two anisotropy fields H_{a1} and H_{a2} , which are the effective anisotropy fields when the magnetization deviates from the easy axis in the hard plane and in the easy plane, respectively. Based on the Landau–Lifshitz–Gilbert (LLG) equation, the resonance frequency $f_r = \gamma(H_{a1}H_{a2})^{1/2}/2\pi$ and the static permeability $\mu_s = 1 + M_s/H_{a2}$, where γ is the gyromagnetic ratio.

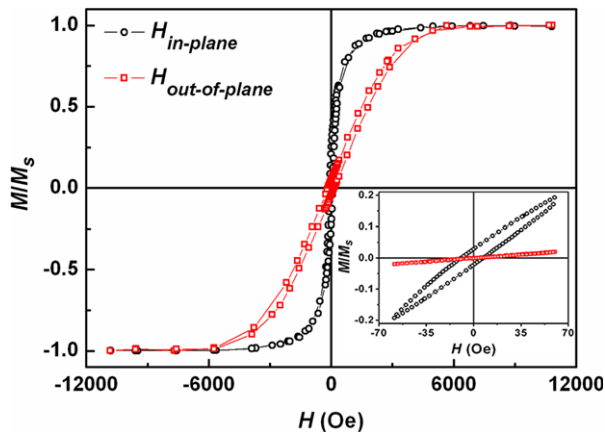


Figure 6. Magnetic hysteresis loop for the $\text{Ni}_x\text{Zn}_{1-x}\text{Fe}_2\text{O}_4$ ($x = 0.45$) thin films with maximum applied field of 12 000 Oe. The inset is the minor loop of this film with maximum applied field of 60 Oe. (Colour online.)

The product of the static permeability and the resonance frequency of the bianisotropy magnetic materials satisfy $(\mu_s - 1)f_r = (\gamma/2\pi)(H_{a1}/H_{a2})^{1/2}M_s$. For the Ni–Zn ferrite bulks, $H_{a1} = H_{a2} = H_k$ (cubic magnetocrystalline anisotropy field). For the films, due to the film plane being the easy magnetizing plane and the hard magnetizing axis being perpendicular to the film plane, $H_{a1} \approx M_s$ (out-of-plane demagnetization field). In the film plane, due to exchange coupling among the nanocrystalline particles, which have magnetocrystalline anisotropy, a relatively smaller effective anisotropy field of H_{a2} (in-plane) was generated [20, 22]. Therefore, the Ni–Zn ferrite thin films can exhibit much higher natural resonant frequency exceeding Snoek's limit of a ferrite bulk.

4. Conclusions

In summary, we successfully fabricated Ni–Zn ferrite films with different compositions by RF magnetron sputtering at room temperature. All the films have well-crystallized spinel structure and exhibit relatively large μ' of 20.5–7 and high f_r of 1.85–4.3 GHz which exceed Snoek's limit for the bulk ferrite samples with the same composition. In particular, the ferrite film with $x = 0.45$ has a large μ' of 15 and a much higher f_r of 2.8 GHz. The reason why the ferrite films have a high f_r can be explained by making use of the bianisotropy model. We could adjust the resonance frequency f_r of the ferrite films by changing the composition to satisfy the practical application.

Since not only μ' but also μ'' of the ferrite films have large values in the gigahertz range, these films will be applicable to planar inductors as well as wave absorbers for suppressing EMI in electronic integrated devices operating in the gigahertz

range. These applications are also greatly promising because of the ferrite films being deposited by sputtering at room temperature. Certainly, the reason that the Ni–Zn ferrite films *in situ* deposited by magnetron sputtering at room temperature have a well-defined spinel structure is being investigated and will be presented in a forthcoming paper.

Acknowledgments

Financial supports by the National Natural Science Foundation of China (NSFC) (No 10774062) and the Keygrant Project of the Chinese Ministry of Education (No 309027) are gratefully acknowledged.

References

- [1] Beji Z, Ammar S, Smiri L S, Vaulay M J, Herbst F, Gallas B and Fiévet F 2008 *J. Appl. Phys.* **103** 07E744
- [2] Subramani A K, Matsushita N, Watanabe T, Kondo K, Tada M, Abe M and Yoshimura M 2008 *J. Appl. Phys.* **103** 07E502
- [3] Sun K, Lan Z, Yu Z, Nie X, Li L and Liu C 2008 *J. Magn. Mater.* **320** 1180
- [4] Shen X, Gong R, Feng Z, Nie Y, Li H and Nie J 2007 *J. Am. Ceram. Soc.* **90** 2196
- [5] Caruntu G, Dumitru I, Bush G G, Caruntu D and O'Connor C J 2005 *J. Phys. D: Appl. Phys.* **38** 811
- [6] Kondo K, Yoshida S, Ono H and Abe M 2007 *J. Appl. Phys.* **101** 09M502
- [7] Liu F, Ren T, Yang C, Liu L, Wang A Z and Yu J 2006 *Mater. Lett.* **60** 1403
- [8] Matsushita N, Chong C P, Mizutani T and Abe M 2002 *J. Appl. Phys.* **91** 7376
- [9] Zuo X, Yang A, Yoon S D, Christodoulides J A, Harris V G and Vittoria C 2005 *Appl. Phys. Lett.* **87** 152505
- [10] Wakiya N, Shinozaki K and Mizutani N 2004 *Appl. Phys. Lett.* **85** 1199
- [11] Bohra M, Prasad S, Kumar N, Misra D S, Sahoo S C, Venkataramani N and Krishnan R 2006 *Appl. Phys. Lett.* **88** 262506
- [12] Koblichka M R, Kirsch M, Brust M, Koblichka-Veneva A and Hartmann U 2008 *Phys. Status Solidi b* **205** 1783
- [13] Desai M, Prasad S, Venkataramani N, Samajdar I, Nigam A K, Keller N, Krishnan R, Baggio-Saitovitch E M, Pujada B R and Rossi A 2002 *J. Appl. Phys.* **91** 7592
- [14] Bae S Y, Kim C S and Oh Y J 1999 *J. Appl. Phys.* **85** 5226
- [15] Liu Y, Chen L, Tan C Y, Liu H J and Ong C K 2005 *Rev. Sci. Instrum.* **76** 063911
- [16] Gao J, Cui Y and Yang Z 2004 *Mater. Sci. Eng. B* **110** 111
- [17] Matsushita N, Abe T, Kondo K, Yoshida S and Abe M 2005 *J. Appl. Phys.* **97** 10G106
- [18] Nakamura T 2000 *J. Appl. Phys.* **88** 348
- [19] Tsutaoka T 2003 *J. Appl. Phys.* **93** 2789
- [20] Abe M, Tada M, Matsushita N and Shimada Y 2006 *J. Appl. Phys.* **99** 08M907
- [21] Xue D, Li F, Fan X and Wen F 2008 *Chin. Phys. Lett.* **25** 4120
- [22] Herzer G. 1990 *IEEE Trans. Magn.* **26** 1397